

# Variability of the Martian ionosphere from the MAVEN Radio Occultation Science Experiment

MeiJuan Yao<sup>1</sup>, Jun Cui<sup>1,2,3\*</sup>, XiaoShu Wu<sup>2,3</sup>, YingYing Huang<sup>1</sup>, and WenRui Wang<sup>1</sup>

<sup>1</sup>School of Atmospheric Sciences, Sun Yat-sen University, Zhuhai Guangdong 519082, China;

<sup>2</sup>National Astronomical Observatories of China, Chinese Academy of Sciences, Beijing 100101, China;

<sup>3</sup>Chinese Academy of Sciences Center for Excellence in Comparative Planetology, Hefei 230026, China

**Abstract:** The Martian ionosphere is produced by a number of controlling processes, including solar extreme ultraviolet radiation (EUV) and X-ray ionization, impact ionization by precipitating electrons, and day-to-night transport. This study investigates the structural variability of the Martian ionosphere with the aid of the radio occultation (RO) experiments made on board the recent Mars Atmosphere and Volatile Evolution (MAVEN) spacecraft. On the dayside, the RO electron density profiles are described by the superposition of two Chapman models, representing the contributions from both the primary layer and the low-altitude secondary layer. The inferred subsolar peak electron densities and altitudes are  $1.24 \times 10^5 \text{ cm}^{-3}$  and 127 km for the former, and  $4.28 \times 10^4 \text{ cm}^{-3}$  and 97 km for the latter, respectively, in general agreement with previous results appropriate for the low solar activity conditions. Our results strengthen the role of solar EUV and X-ray ionization as the driving source of plasma on the dayside of Mars. Beyond the terminator, a systematic decline in ionospheric total electron content is revealed by the MAVEN RO measurements made from the terminator crossing up to a solar zenith angle of 120°. Such a trend is indicative of day-to-night plasma transport as an important source for the nightside Martian ionosphere.

**Keywords:** Mars; planetary ionospheres; radio occultation

**Citation:** Yao, M. J., Cui, J., Wu, X. S., Huang, Y. Y., and Wang, W. R. (2019). Variability of the Martian ionosphere from the MAVEN Radio Occultation Science Experiment. *Earth Planet. Phys.*, 3(4), 283–289. <http://doi.org/10.26464/epp2019029>

## 1. Introduction

The dayside Martian ionosphere contains a well-defined primary layer (hereafter denoted as  $M_2$ ) and a low-altitude secondary layer (hereafter denoted as  $M_1$ ), which are frequently depicted as analogous to the terrestrial F and E layers (Mendillo et al., 2003; Rishbeth and Mendillo, 2004). These layers are mainly produced by solar extreme ultraviolet radiation (EUV) and X-ray ionization along with impact ionization by photoelectrons and their secondaries (Withers, 2009 and references therein). Their structures are reasonably well described by the idealized Chapman theory, varying systematically with both the solar zenith angle (SZA) and the solar ionizing flux (e.g., Hantsch and Bauer, 1990; Martinis et al., 2003; Withers and Mendillo, 2005; Fox and Yeager, 2006, 2009; Nielsen et al., 2006; Morgan et al., 2008; Fox and Weber, 2012).

On the nightside, the Martian ionosphere is patchy and sporadic, with electron precipitation generally thought to be the dominant source of ionization (e.g., Verigin et al., 1991; Safaeinili et al., 2007; Fowler et al., 2015; Girazian et al., 2017a). In practice, energetic electrons capable of ionizing the nightside Martian atmosphere could be either solar wind electrons or photoelectrons produced on the dayside and transported to the nightside under favorable ambient magnetic field configurations (Xu SS et al., 2016, 2017;

Weber et al., 2017; Adams et al., 2018). In addition, horizontal transport has been suggested as a viable mechanism supporting a nightside ionosphere on Mars, especially near the terminator (e.g., Zhang et al., 1990; Němec et al., 2010; Duru et al., 2011; Withers et al., 2012a; Cui J et al., 2015a; Girazian et al., 2017b).

A significant amount of information on the structural variability of the Martian ionosphere comes from a large collection of vertical electron density profiles acquired by the Radio Occultation (RO) Science Experiments (e.g., Withers, 2009 and references therein). Such experiments have been made on board the Mariner 9, Mars Orbiter, Vikings 1 and 2, Mars Global Surveyor (MGS), and Mars Express (MEx), among others (e.g., Kliore et al., 1972, 1973; Lindal et al., 1979; Tyler et al., 1992, 2001; Hinson et al., 1999; Pätzold et al., 2005, 2016). With such a technique, the radio links between the orbiters and the ground-based telescopes on Earth are used to measure the signal variations caused by changes in the local refractivity of the Martian ionosphere (e.g., Withers et al., 2014). Radio occultation experiments were also made on board the recent Mars Atmosphere and Volatile Evolution (MAVEN; Jakosky et al., 2015). With the release of the MAVEN RO electron density profiles, it is an opportune time to investigate the variability of the Martian ionosphere further with these new data sets and compare them with early results.

## 2. Data Description

The MAVEN RO Science Experiment is a two-way, single-fre-

Correspondence to: J. Cui, cuijun7@mail.sysu.edu.cn

Received 25 MAR 2019; Accepted 17 APR 2019.

Accepted article online 09 MAY 2019.

©2019 by Earth and Planetary Physics.

quency (at X-band) RO experiment that provides information on the vertical electron density profiles in the Martian ionosphere. The analysis presented here relies exclusively on the MAVEN RO measurements made from 5 Jul 2016 to 13 Oct 2018, a period under solar minimum conditions and covering the entire surface of Mars over an SZA range of 54°–131°. Information on the solar EUV and X-ray irradiance is available from the MAVEN Extreme Ultraviolet Monitor (EUVM) measurements (Eparvier et al., 2015); thus, extrapolation from the near-Earth measurements, as required by previous analyses of the Mars aeronomical data (Withers, 2009 and references therein), is no longer necessary. Here, with the aid of the EUVM Level 3 solar spectral model at Mars constructed from the Flare Irradiance Spectral Model for Mars and calibrated with the EUVM band irradiance data (Thiemann et al., 2017), we estimate the integrated solar energy flux shortward of 89.8 nm, corresponding to the energy range above the nominal CO<sub>2</sub> ionization potential of 13.8 eV (Bhardwaj and Jain, 2009), as 0.75–1.5

erg·cm<sup>-2</sup>·s<sup>-1</sup>.

For reference, in Figure 1 we provide the distributions of the available RO measurements with respect to longitude and latitude in the left panel and with respect to the SZA and solar ionizing flux in the right panel. All geophysical parameters in the figure refer to the values at the closest approach of the downlink ray. Because the majority of the available RO measurements were made at an SZA below 120° (with only eight individual profiles in the range of 120°–135°), here we restrict our analysis of the ionospheric variability on Mars to the dayside and the cross-terminator regions only. For reference, the MGS RO measurements cover an SZA range of 70°–90°, whereas the MEx RO measurements cover an SZA range of 50°–120°, in comparison with the maximum possible SZA range of 44°–136° potentially sampled by the RO technique (Gurnett et al., 2008).

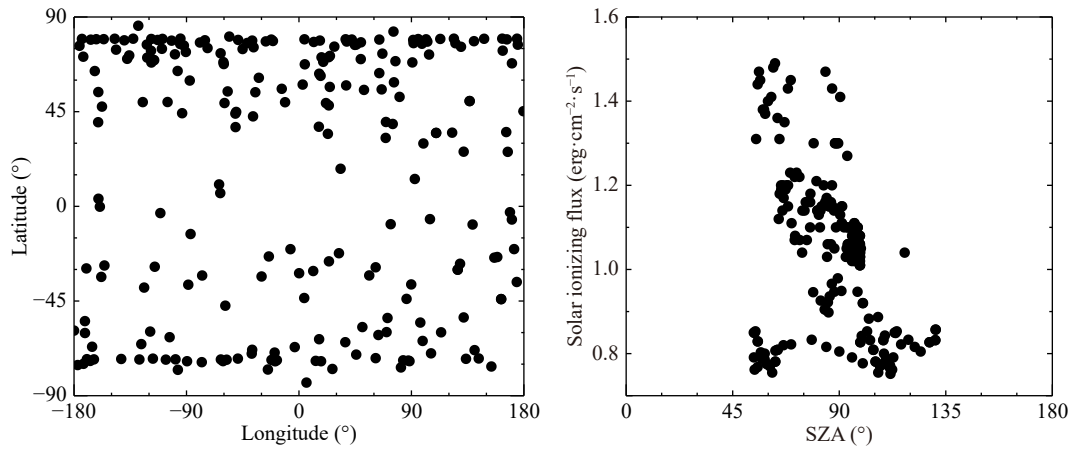


**Figure 1.** Distributions of the available MAVEN RO measurements from 5 Jul 2016 to 13 Oct 2018 with respect to longitude and latitude in the left panel, and with respect to the SZA and solar ionizing flux in the right panel. All geophysical parameters refer to the values at the closest approach of the downlink ray. The solar ionizing flux is obtained by integrating the MAVEN Extreme Ultraviolet Monitor (EUVM) solar spectral model shortward of 89.8 nm. Each point in the figure represents an individual electron density profile.

### 3. Variability of the Martian Ionosphere

#### 3.1 The Dayside Martian Ionosphere

Several representative electron density profiles on the dayside of Mars are displayed in Figure 2 in order of increasing SZA from left to right. All manifest as a regular morphology with a pronounced primary layer lying on top of a secondary layer, with the latter typically appearing as a mere shoulder (e.g. Withers, 2009). The MAVEN RO measurements reveal dayside variability in terms of the presence or absence of a clearly identified ionopause (Vogt et al., 2015), the flatness or sharpness of the primary peak (Withers et al., 2012b), and the emergence of transient layers (Kopf et al., 2008), among others. Overlying such variability is the ordered trend of decreasing peak electron density and increasing peak electron altitude, both with an increasing SZA.

To investigate the variations in the primary and secondary layers, we used the sum of two idealized Chapman functions to model the measured electron density profile, where each Chapman function characterizes the contribution of an individual layer, either M<sub>2</sub>

or M<sub>1</sub>. Kopf et al. (2008) used a similar approach based on the sum of several Gaussian functions to describe the superposition of multiple layer structures present in the dayside Martian ionosphere. Our approach involves six independent free parameters, including the peak electron densities and altitudes, as well as the respective neutral-density scale heights for both layers, which are constrained by data-model comparison with the aid of the traditional Levenberg–Marquardt least-squares fitting algorithm. The appropriate functional form can be written as

$$N_e = \sum_{i=1}^2 N_{im} \exp \left\{ \frac{1}{2} \left[ 1 - \frac{z - z_{im}}{H_i} - \exp \left( -\frac{z - z_{im}}{H_i} \right) \right] \right\}, \quad (1)$$

where  $N_e$  is the electron number density, and  $N_{im}$ ,  $z_{im}$ , and  $H_i$  are the peak electron density, peak electron altitude, and appropriate neutral density scale height, respectively, for layer  $i$  (2 for the primary layer and 1 for the secondary layer following the conventional nomenclature). The data-model comparison is restricted to regions typically extending above the primary peak for several tens of kilometers because the electron distribution at higher alti-

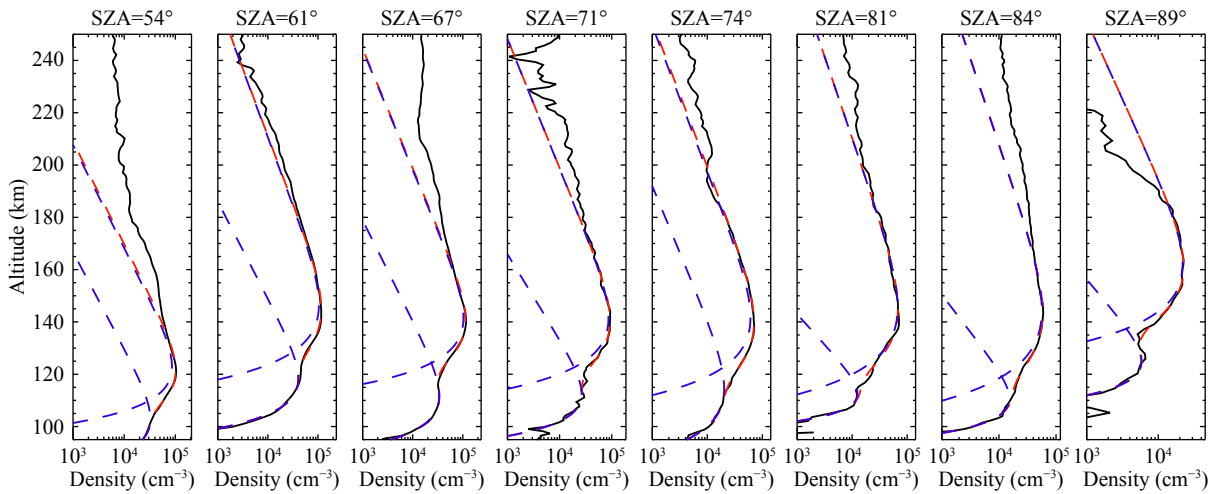


**Figure 2.** Representative electron density profiles of the dayside Martian ionosphere based on the MAVEN RO measurements (solid black lines), along with the double Chapman model fits (dashed red lines), in order of increasing SZA from left to right. The respective contributions of the  $M_2$  and  $M_1$  layers are indicated by dashed blue lines for reference.

tudes is known to be dynamically controlled rather than photochemically controlled, either under diffusive equilibrium (e.g., Martinis et al., 2003; Fox and Yeager, 2006; Matta et al., 2015) or subject to bulk ion outflow (e.g., Fox, 1997, 2009; Wu WS et al., 2019). Note that the condition of photochemical equilibrium is an underlying assumption of the idealized Chapman theory (Chapman, 1931a, b). Under some circumstances, a portion of the measured electron density profile well below the secondary peak is also excluded from the data-model comparison because of the potential presence of a meteoric layer (e.g., Pätzold et al., 2005; Withers et al., 2008; Schneider et al., 2015). In practice, the altitude range used for the double Chapman model fitting is determined manually for each individual electron density profile examined here. The upper boundary is typically placed at 180 km above the surface, where we could estimate a chemical loss time constant of 600 s via dissociative recombination (e.g., Peverall et al., 2001), assuming a reference electron density of  $10^4 \text{ cm}^{-3}$  (see Figure 2) and reference electron temperature of 500 K (Ergun et al., 2015; Cui J et al., 2015b). For comparison, the plasma diffusion time constant is comparable, with a reference ion-neutral colli-

sion frequency of  $1 \text{ s}^{-1}$  (Schunk, 1977), a reference background neutral density of  $10^9 \text{ cm}^{-3}$ , and a reference neutral density scale height of 10 km (Mahaffy et al., 2015). For the profiles displayed in Figure 2, the best-fit model results are superimposed on the red solid lines for comparison, and the respective contributions of the two layers are indicated by the dashed blue lines.

The SZA variations of the best-fit peak electron densities and altitudes are displayed in Figure 3, with red indicating  $M_2$  and blue indicating  $M_1$ , respectively, in agreement with the prediction of the solar-driven scenario. The variations for the  $M_2$  layer can be reasonably described by

$$z_{2m} = 1.24 \times 10^5 (\cos \theta)^{0.39} \text{ cm}^{-3}, \quad (2)$$

$$z_{2m} = 127 - 9.3 \times \ln(\cos \theta) \text{ km}, \quad (3)$$

where  $\theta$  is the SZA. Equations (2a) and (2b) predict a subsolar peak electron density of  $1.24 \times 10^5 \text{ cm}^{-3}$  at 127 km. In comparison, Hantsch and Bauer (1990) found the subsolar  $M_2$  peak to be  $2 \times 10^5 \text{ cm}^{-3}$  at 120 km based on pre-MGS RO measurements, Fox and Yeager (2009) and Fox and Weber (2012) found it to be  $1.5 \times$

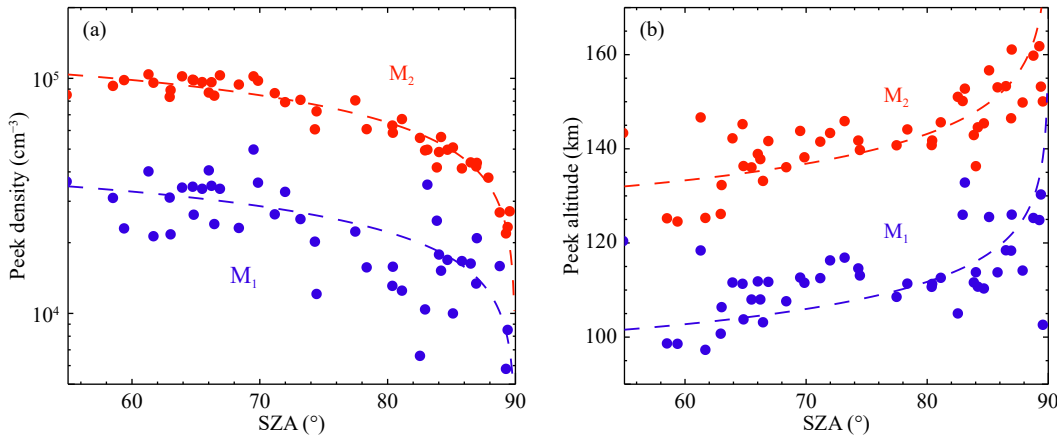


**Figure 3.** SZA variations of the best-fit peak electron densities (a) and peak electron altitudes (b) based on the available MAVEN RO measurements. Red indicates the  $M_2$  layer, and blue indicates the  $M_1$  layer, respectively.

$10^5 \text{ cm}^{-3}$  at 126 km based on MGS RO measurements, [Zhang SJ et al. \(2015\)](#) found it to be  $1.5 \times 10^5 \text{ cm}^{-3}$  at 128 km based on MEx RO measurements, and [Morgan et al. \(2008\)](#) found it to be  $1.6 \times 10^5 \text{ cm}^{-3}$  at 134 km based on MEx MARSIS measurements in the active ionospheric sounding mode.

The largest discrepancy was encountered when comparing our result with an early investigation by [Hantsch and Bauer \(1990\)](#), whose  $M_2$  peak electron density at subsolar conditions was higher than our value by 60%. Such a discrepancy is not surprising, given that the analysis of [Hantsch and Bauer \(1990\)](#) was made with pre-MGS RO data accumulated over a wide range, with a 10.7 cm solar radio index of 70 to 200 solar flux units (SFU,  $10^{-22} \text{ W m}^{-2} \text{ Hz}^{-1}$ ), whereas the available MAVEN RO data were gathered exclusively under low solar activity conditions with a mean 10.7 cm solar radio index of 75 SFU. Because the MEx RO and MARSIS data were also acquired under low solar activity conditions, the subsolar peak electron density for  $M_2$  in the present study is in general agreement with the earlier analyses of [Zhang SJ et al. \(2015\)](#) and [Morgan et al. \(2008\)](#). In addition, we should emphasize that the MGS RO measurements were made over a wide range, with a 10.7 cm solar radio index of 80 to 200 SFU. However, the subsolar peak electron density for  $M_2$  quoted above has been corrected for the solar cycle variation and is appropriate for a MAVEN equivalent mean 10.7 cm solar radio index of 75 SFU. Regarding the subsolar peak electron altitude for  $M_2$ , our results were in general agreement with various studies and the typical difference was only several kilometers. This result indicates that the solar ionizing flux influences the peak electron density more prominently than the peak electron altitude. For a direct comparison with our result, the MGS subsolar peak electron altitude of 126 km found by [Fox and Weber \(2012\)](#) represents the value averaged over different longitudinal bins and weighted by the respective numbers of available RO electron density profiles in these bins. A systematic longitudinal pattern, manifesting as a strong wave-3 feature, is well known to be present on Mars and is thought to be linked to the nonmigrating tidal waves in the ambient neutral atmosphere (e.g., [Bougher et al., 2001, 2004](#)), but such a feature cannot be confirmed by the longitudinally averaged analysis presented here and is left for follow-up studies.

Similarly, the SZA variations for the  $M_1$  layer under solar minimum conditions, as inferred from the MAVEN RO measurements, can be described by

$$N_{1m} = 4.28 \times 10^4 (\cos \theta)^{0.38} \text{ cm}^{-3}, \quad (4)$$

$$z_{1m} = 97 - 8.5 \times \ln(\cos \theta) \text{ km}, \quad (5)$$

predicting a subsolar peak electron density of  $4.28 \times 10^4 \text{ cm}^{-3}$  at 97 km. By comparison, [Fox and Yeager \(2009\)](#) and [Fox and Weber \(2012\)](#) found such a peak to be located at a longitudinally averaged altitude of 108 km with a peak density of  $5.5 \times 10^4 \text{ cm}^{-3}$  appropriate for a mean 10.7 cm solar radio index of 75 SFU. Although the subsolar peak electron densities for  $M_1$  from the two works are in reasonable agreement, the relatively large discrepancy in the subsolar peak electron altitude (by 11 km) is likely indicative of the difficulty of separating the contribution of the weak and noisy  $M_1$  layer from the total electron density profile.

Except close to the terminator, the SZA variations of the peak electron densities for both layers vary ideally with  $(\cos \theta)^{0.5}$  according to the Chapman theory (e.g., [Morgan et al., 2008](#)), but in practice, the two power indexes are usually found to be substantially different from 0.5 because of the inherent approximations in the Chapman theory ([Chapman, 1931a, b](#)). Here, the power indexes were estimated to be nearly 0.4 for both layers based on the MAVEN RO data and are broadly consistent with the 0.45 for  $M_2$  and 0.39 for  $M_1$  reported by [Fox and Yeager \(2009\)](#) based on MGS RO measurements.

Finally, we note that the dayside averaged neutral density scale heights implied by equations (2) and (3) were 9.3 km and 8.5 km, respectively, around the  $M_2$  and  $M_1$  peaks. These values were different from previous estimates by  $\pm 30\%$ : 10 km reported by [Hantsch and Bauer \(1990\)](#) based on pre-MGS RO measurements, 6.8 km for  $M_2$  and 4.2 km for  $M_1$  by [Fox and Weber \(2012\)](#) based on MGS RO measurements, and 12.9 km by [Morgan et al. \(2008\)](#) based on MEx MARSIS measurements, where the MGS values were again obtained by averaging over different longitudinal bins. Provided that the scale height obtained from Chapman fitting is a useful diagnostic for the ambient neutral temperature, we would expect the pre-MGS and MGS values, which characterize both low and high solar activity conditions, to be higher than the MEx and MAVEN values, which characterize exclusively low solar activity conditions (e.g., [Jain et al., 2015; Bougher et al., 2017](#)), but this is clearly not the case. As discussed by [Cui J et al. \(2015b\)](#), the scale height from Chapman fitting does not necessarily represent the true neutral density scale height because of the nonnegligible contribution of a positive electron temperature gradient, in comparison with the constant electron temperature assumed in the Chapman theory ([Chapman, 1931a, b](#)). In practice, a steep electron temperature gradient is present near the ionospheric peak on Mars according to both numerical calculations (e.g., [Chen RH et al., 1978; Choi et al., 1998; Matta et al., 2014](#)) and spacecraft in situ measurements (e.g., [Hanson and Mantas, 1988; Ergun et al., 2015; Flynn et al., 2017](#)).

### 3.2 The Cross-terminator Martian Ionosphere

Approximately half of the available MAVEN RO electron density profiles are located within the SZA range of  $90^\circ$ – $120^\circ$ , providing a sufficiently large sample for investigating the morphological variability of the cross-terminator Martian ionosphere. Several representative profiles are presented in [Figure 4](#) in order of increasing SZA from left to right. The figure reveals a considerably larger variability as compared with the dayside, which strengthens the earlier conclusion that the Martian ionosphere beyond the terminator is patchy and sporadic (e.g., [Gurnett et al., 2008](#)). Yet unlike the dayside, not all profiles present distinctive layer structures; accordingly, we did not attempt Chapman fits to the electron density profiles beyond the terminator. Instead, the variation in the cross-terminator Martian ionosphere was investigated in terms of the total electron content (TEC) obtained by the column integrating the measured electron density profiles.

The SZA variation of the ionospheric TEC beyond the terminator is displayed in [Figure 5](#) over an SZA range of  $90^\circ$ – $120^\circ$ . At the terminator crossing, the TEC derived from the RO density profiles

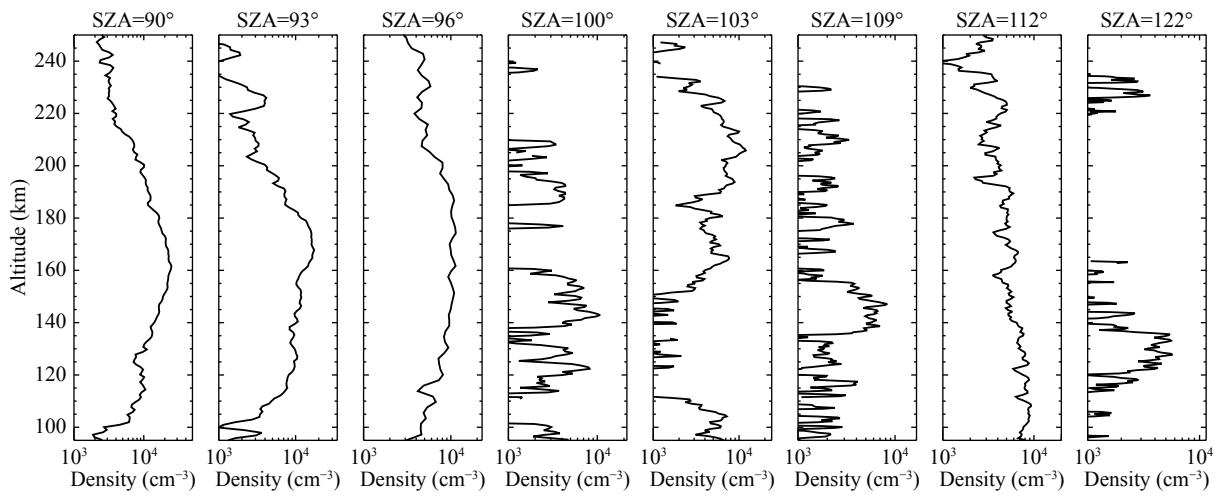


**Figure 4.** Representative electron density profiles of the cross-terminator Martian ionosphere based on MAVEN RO measurements, in order of increasing SZA from left to right.

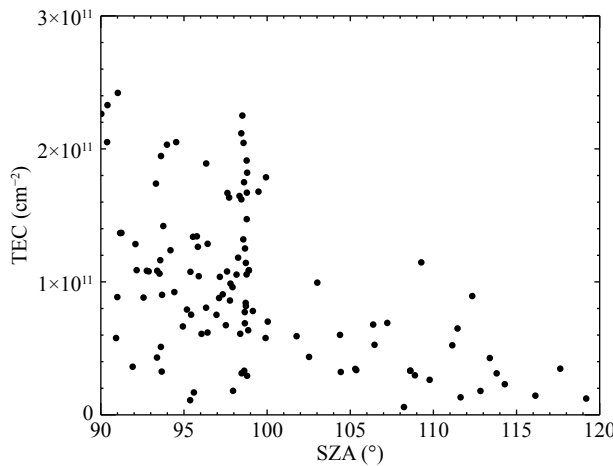


**Figure 5.** SZA variation of the ionospheric TEC on Mars over an SZA range of 90°–120°.

typically lies over a range of  $(1-2) \times 10^{11} \text{ cm}^{-2}$ , consistent with MARSIS subsurface measurements (e.g., Cui J et al., 2015a). Despite the considerable scattering as compared with the dayside SZA variation (see Figure 3), the nightside RO data suggest the appearance of a general trend, with the TEC decreasing systematically beyond the terminator crossing. Such behavior is consistent with previous results obtained from the pre-MGS RO data (Zhang SJ et al., 2015), the MEx RO data (Withers et al., 2012a), and the MEx MARSIS data in both the active ionospheric sounding mode (Němec et al., 2010; Duru et al., 2011) and the subsurface mode (Cui J et al., 2015a). This trend should reflect the combined effect of solar EUV and X-ray ionization, which does not decline to become nonnegligible beyond the terminator because of the finite thickness of the Martian atmosphere, and day-to-night transport, which manifests as a continuous depletion of the ionospheric plasma content by dissociative recombination as Mars rotates into the darkness. At an even larger SZA, we would expect the ionospheric TEC on Mars to remain at a roughly constant level in response to solar wind electron precipitation as the dominant source of ionization and to be independent of the SZA (Withers et

al., 2012; Cui J et al., 2015a). However, only eight individual RO electron density profiles are available at an  $\text{SZA} > 120^\circ$ , which does not allow for rigorous evaluation of the role of electron precipitation.

#### 4. Concluding Remarks

The RO experiments provide useful information on the electron density profiles throughout the Martian ionosphere by using radio links between the orbiters and the ground-based telescopes to measure the signal variations caused by changes in the local refractivity of the ionosphere (e.g., Withers et al., 2014). Like the previous RO experiments conducted on board the Mariner 9, Mars Orbiter, Vikings 1 and 2, MGS, and MEx, the MAVEN RO measurements provide a useful data set for examining the ionospheric variability on Mars. In this study, we analyzed the available MAVEN RO electron density profiles, which covered an SZA range of up to  $120^\circ$ . On the dayside, we modeled the measured electron density profiles with the superposition of two Chapman functions to include the contributions of both the primary  $M_2$  layer and the low-altitude  $M_1$  layer (Mendillo et al., 2003; Rishbeth and Mendillo, 2004). On the nightside, we parameterized the measured electron density profiles by using the respective TEC values.

Our analysis generally confirms the solar-driven scenario for the dayside Martian ionosphere. The SZA variations in the peak electron densities and peak electron altitudes for both layers are in agreement with predictions by the idealized Chapman theory (Chapman, 1931a, b). The inferred subsolar peak electron densities are  $1.24 \times 10^5 \text{ cm}^{-3}$  at 127 km for  $M_2$  and  $4.28 \times 10^4 \text{ cm}^{-3}$  at 97 km for  $M_1$ , appropriate for low solar activity conditions with a mean 10.7 cm solar radio index of 75 SFU. These values are consistent with previous values found from different data sets and under similar solar activity conditions (e.g., Morgan et al., 2008; Fox and Yeager, 2009; Fox and Weber, 2012; Zhang SJ et al., 2015). The dominant role of solar wind electron precipitation on the deep nightside of Mars (e.g., Verigin et al., 1991; Safaeinili et al., 2007; Fowler et al., 2015; Girazian et al., 2017a) will need to be examined further as more RO electron density profiles are accumulated at an  $\text{SZA} > 120^\circ$ .



